IEEE/RSJ International Conference on Intelligent Robots and Systems, Detroit, USA, 2023.

Autonomous ultrasound scanning towards standard plane using interval interaction probabilistic movement primitives

Yi Hu[1] and Mahdi Tavakoli[1]

***Abstract*— Learning from demonstrations is the paradigm where robots acquire new skills demonstrated by an expert and alleviate the physical burden on experts to perform repetitive tasks. Ultrasound scanning is one of the ways to view the anatomical structures of soft tissues, but it is repetitive for some tissue scanning tasks. In this study, an autonomous ultrasound scanning towards a standard plane framework is proposed. Interaction probabilistic movement primitives (iProMP) was proposed for the collaborative tasks for human and robot movement. Inspired by the interval type-2 fuzzy system, an interval iProMP is proposed to learn the ultrasound scanning navigation strategy from scanning demonstrations and the collaborative agents are the robot movement and ultrasound image information. The proposed interval iProMP improves the capacity of dealing with uncertainties due to insufficient observations during reproduction. U-Net is applied to recognize the desired ultrasound image shown during demonstrations and a confidence map is used to evaluate the ultrasound image quality. Breast seroma scanning is chosen as the ultrasound scanning task to validate the performance of the proposed autonomous ultrasound scanning framework. Ultrasound navigation is to realize autonomous ultrasound scanning for localizing the breast seroma. The simulation comparison result shows the better performance of the proposed interval iProMP under insufficient observation, compared to traditional iProMP. The experiment result validates the feasibility and generality of the proposed autonomous ultrasound scanning framework using interval iProMP with a higher success rate than that with traditional iProMP.**

I. Introduction

Learning from demonstrations (LfD) provides an effective way to help humans transfer various complicated skills to robots without any programming experience. Based on the operation demonstrations by humans, robots can acquire and later automatically implement desired tasks. LfD has been widely used in different fields, such as physical rehabilitation [1], highway driving [2], drilling [3], and re-grasping object [4], LfD has been used in the field of autonomous surgery for suturing [5] and retraction [6].

Clinical diagnosis incorporates ultrasound scanning as an essential component. Based on their extensive experience, clinicians utilize the US probe to locate desired anatomical structures and planes. The US standard plane represents the desired US image slice and serves as the scanning objective in the US scanning process. However, certain US scanning tasks are repetitive and can strain clinicians physically. Leveraging LfD can effectively transfer expert skills to robots, allowing for reducing the physical burden on clinicians.

There developed some research on autonomous US scanning towards standard a plane using LfD. In [7], the robotic US scanning skill, including the US image features, the pose/position of the probe, and contact force, was encapsulated into a high-dimensional multi-modal model and trained by a deep neural network to learn the skill from experience. In [8], a procedure-specified imitation learning framework was proposed to realize autonomous scanning for both in-plane and out-of-plane feature tasks in the targeted carotid artery examination procedure. Inverse optimal control or reinforcement learning is a popular method used in LfD by inferring reward functions. Burke et al. applied a probabilistic temporal ranking strategy to learn rewards from demonstration image sequences containing exploratory actions [9].

However, training a deep neural network to predict the US probe movement based on image features is time-consuming and has high computational complexity. Reinforcement learning attracts more and more attention in the field of LfD, but it is not easy to find and design an appropriate reward function to infer the relationship between US probe movement and US image feature. Probabilistic movement primitives (ProMP), proposed in 2013, is one of the most widely used methods for LfD that parametrizes the human demonstration distribution by a Hierarchical Bayesian Model and allows for the derivation of new operations [10]. In [11], iProMP was proposed for collaborative and assistive robots to infer the corresponding movement from the recognition of different human actions. Fuzzy set theory was proposed by Zadeh in 1965 and crisp membership functions of the type-1 fuzzy system (T1FS) characterized fuzziness for describing the degree of membership [12]. Interval type-2 fuzzy system (IT2FS) has been proven to obtain better performance than T1FS in dealing with nonlinear and uncertain models due to the nature of its interval membership function, also called the footprint of uncertainty (FOU). The membership function of IT2FS is an interval area that covers a broader spectrum of uncertainty and nonlinearity. Inspired by the FOU of IT2FS, in this study, an interval iProMP is proposed as developed, in which an adaptive factor α is designed to obtain an adaptive modulation between the upper and lower predicted trajectories generated by the proposed interval iProMP and can be adaptive updated based on the prediction differences of trajectory at each observation.

Overall, the motivation of this paper is to realize automa-

*This research was supported by the Natural Sciences and Engineering Research Council (NSERC) of Canada and the China Scholarship Council (CSC).

[1]Yi Hu and Mahdi Tavakoli are with the Department of Electrical and Computer Engineering, Faculty of Engineering, University of Alberta, Edmonton T6G 1H9, Alberta, Canada. Email: {hu19, mahdi.tavakoli}@ualberta.ca

tion in US scanning tasks and reduce the physical burden on clinicians. Although there have developed some research on autonomous US scanning using deep neural networks and reinforcement learning, the high computational complexity is a problem that cannot be ignored. In this paper, autonomous US scanning towards a standard plane framework is proposed using interval iProMP. The proposed interval iProMP is used to learn the collaborative interaction trajectories of robot movement and US image information. U-Net will be applied to extract US image features that infer the scanning strategy. The US image quality will be evaluated by a confidence map.

To validate the feasibility and generality of the proposed autonomous US scanning framework, breast seroma scanning is selected as the US scanning task in the experiment. Lumpectomy is a kind of breast-conserving surgery and after removing breast cancer, the area occupied by cancer before may develop a serous fluid collection called a seroma. The US scanning task of breast seroma in the experiment is to localize the seroma in the center of the US image. Based on the above discussion, the contributions of this study are as follows: 1) Inspired by the advantages of FOU in IT2FS, an interval iProMP is proposed to improve the capacity of modeling the weight of trajectories and dealing with insufficient observations during reproduction; 2) An adaptive factor α is proposed to obtain an adaptive modulation between the upper and lower predicted trajectories. The updated law of α is designed based on the prediction differences at each observation.

II. Ultrasound Scanning Skills Modeling

In this section, an interval iProMP is proposed to model the weight of demonstration trajectories and a factor $\boldsymbol{\alpha}$ is designed to obtain an adaptive modulation for the crisp output of the predicted trajectory. To model the US scanning skill from demonstrations, the robot movement and US image information are the collaborative agents in interval iProMP.

A. Interaction Probabilistic Movement Primitives

In the iProMP, the probability distribution of interaction trajectories is modeled in lower dimensional weight space. Different from ProMP, iProMP concatenates the weights of the trajectory in a row vector and constructs a block diagonal observation matrix. iProMP is able to generate and predict the movement primitive of the unobserved agent based on observations.

Let us consider human movement as P DOFs which is represented as $(.)^H$ and robot movement as Q DOFs which is represented as $(.)^R$. Therefore, each human-robot collaborative demonstration contains $P+Q$ trajectories. Define each demonstration at time t as the state vector as follows

$$\boldsymbol{y_t} = [y^H_{1,t}, \ldots, y^H_{P,t}, y^R_{1,t}, \ldots, y^R_{Q,t}]^T \tag{1}$$

In the iProMP, a smooth trajectory of length T is assumed to be in a lower dimensional weight space and can be achieved by linear ridge regression on Gaussian basis functions [11]. At time t, a parameterization of trajectory $\boldsymbol{y_t}$ can be represented as

$$\boldsymbol{y_t} = \boldsymbol{H}_t^T \boldsymbol{\omega} + \boldsymbol{\epsilon_y} \tag{2}$$

$$p(\boldsymbol{y}_t|\boldsymbol{\omega}) = \mathcal{N}(\boldsymbol{y}_t|\boldsymbol{H}_t^T\boldsymbol{\omega}, \boldsymbol{\Sigma}_y) \tag{3}$$

where $\boldsymbol{H}_t^T = diag(\boldsymbol{\Psi}_t^T, \ldots, \boldsymbol{\Psi}_t^T)$ is the observation matrix in which Ψ_t is a time-dependent basis function at time t and $\boldsymbol{\epsilon_y} \sim \mathcal{N}(\mathbf{0}, \boldsymbol{\Sigma_y})$ is the zero-mean i.i.d Gaussian noise. The observation matrix $\boldsymbol{H}_t^T$ consists of observed basis functions for humans and unobserved for robot as follows

$$\boldsymbol{H}_t^T = \left[\begin{array}{ccc:ccc} (\boldsymbol{\Psi}_t^H)^T & \cdots & \mathbf{0} & \mathbf{0} & \cdots & \mathbf{0} \\ \mathbf{0} & \ddots & \mathbf{0} & \mathbf{0} & \ddots & \mathbf{0} \\ \mathbf{0} & \cdots & (\boldsymbol{\Psi}_t^H)^T & \mathbf{0} & \cdots & \mathbf{0} \\ \hdashline \mathbf{0} & \cdots & \mathbf{0} & \mathbf{0}^R & \cdots & \mathbf{0} \\ \mathbf{0} & \ddots & \mathbf{0} & \mathbf{0} & \ddots & \mathbf{0} \\ \mathbf{0} & \cdots & \mathbf{0} & \mathbf{0} & \cdots & \mathbf{0}^R \end{array}\right] \tag{4}$$

The probability of observing a trajectory $y_{1:T}$ is

$$p(\boldsymbol{y}_{1:T}|\boldsymbol{\omega}) = \prod_1^T \mathcal{N}(\boldsymbol{y}_t|\boldsymbol{H}_t^T\boldsymbol{\omega}, \boldsymbol{\Sigma}_y) \tag{5}$$

The weights can be estimated by a linear ridge regression with the ridge factor λ as follows:

$$\boldsymbol{\omega} = (\boldsymbol{H}^T\boldsymbol{H} + \lambda \boldsymbol{I})^{-1}\boldsymbol{H}^T\boldsymbol{y}_{1:T} \tag{6}$$

The distribution of $\boldsymbol{p(\omega;\theta)}$ is modeled as a Gaussian with mean $\boldsymbol{\mu_\omega} \in \mathbb{R}^N$ and covariance $\boldsymbol{\Sigma_\omega} \in \mathbb{R}^{N\times N}$ and the parameter $\boldsymbol{\theta} = \{\boldsymbol{\mu_\omega}, \boldsymbol{\Sigma_\omega}\}$ is defined to control the distribution of weights.

$$p(\boldsymbol{\omega};\boldsymbol{\theta}) = \mathcal{N}(\boldsymbol{\omega}|\boldsymbol{\mu}_\omega, \boldsymbol{\Sigma}_\omega) \tag{7}$$

The probability of trajectory $p(\boldsymbol{y}_t;\boldsymbol{\theta})$ at time t can be obtained by integrating out the weights

$$\begin{aligned} p(\boldsymbol{y}_t;\boldsymbol{\theta}) &= \int p(\boldsymbol{y}_t|\boldsymbol{\omega})p(\boldsymbol{\omega};\boldsymbol{\theta})d\boldsymbol{\omega} \\ &= \mathcal{N}(\boldsymbol{y}_t|\boldsymbol{H}_t{}^T\boldsymbol{\mu}_\omega, \boldsymbol{H}_t^T\boldsymbol{\Sigma}_\omega\boldsymbol{H}_t + \boldsymbol{\Sigma}_y) \end{aligned} \tag{8}$$

Hence, the distribution of trajectory can be updated by the weights. Given a new desired point, the new mean and covariance of weights can be computed to update the distribution of trajectory.

B. Interval Interaction Probabilistic Movement Primitives

Estimating and modeling the weights of demonstration trajectories are of crucial importance in the learning performance of iProMP. The demonstration weights can be computed by linear ridge regression with the pre-defined basis function. Hence, basis functions and the value of the ridge factor λ are critical in estimating the weights of demonstration trajectories. The fuzzy model of IT2FS can be considered as a collection of multiple T1FS as shown in Fig.1. The FOU of IT2FS helps to cover a broader spectrum of uncertainty and nonlinearity. Inspired by the FOU of IT2FS, in the proposed interval iProMP, the upper

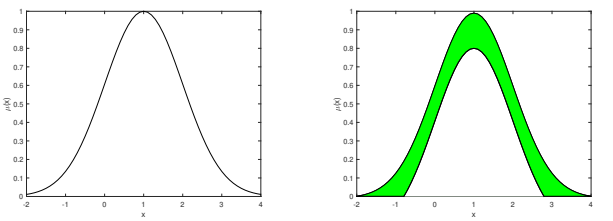

(a) Type-1 fuzzy system (b) Interval type-2 fuzzy system

Fig. 1. Membership function of fuzzy system

and lower basis functions are used to model the weights of demonstration trajectories.

Consider the human-robot collaborative demonstration trajectory at time t

$$\boldsymbol{y}_t = [y^H_{1,t}, \ldots, y^H_{P,t}, y^R_{1,t}, \ldots, y^R_{Q,t}]^T \tag{9}$$

In the interval iProMP, upper and lower basis functions are used to model the demonstration trajectories. Thus, at time t, we have

$$\boldsymbol{y}_t = \overline{\boldsymbol{H}}_t^T \overline{\boldsymbol{\omega}} + \overline{\boldsymbol{\epsilon}}_y \tag{10}$$

$$\boldsymbol{y}_t = \underline{\boldsymbol{H}}_t^T \underline{\boldsymbol{\omega}} + \underline{\boldsymbol{\epsilon}}_y \tag{11}$$

where $\overline{\boldsymbol{\omega}}$ and $\underline{\boldsymbol{\omega}}$ are the upper and lower weights. $\overline{\boldsymbol{H}}_t^T = diag(\overline{\boldsymbol{\Psi}}_t^T, \ldots, \overline{\boldsymbol{\Psi}}_t^T)$ and $\underline{\boldsymbol{H}}_t^T = diag(\underline{\boldsymbol{\Psi}}_t^T, \ldots, \underline{\boldsymbol{\Psi}}_t^T)$ are upper and lower observation matrices, in which $\overline{\boldsymbol{\Psi}}_t$ and $\underline{\boldsymbol{\Psi}}_t$ are the upper and lower basis functions at time t. $\overline{\boldsymbol{\epsilon}} \sim \mathcal{N}(\boldsymbol{0}, \overline{\boldsymbol{\Sigma}}_y)$ and $\underline{\boldsymbol{\epsilon}} \sim \mathcal{N}(\boldsymbol{0}, \underline{\boldsymbol{\Sigma}}_y)$ are zero-mean i.i.d Gaussian noise.

Thus, the distribution of the trajectory at time t can be represented as

$$p(\boldsymbol{y}_t|\overline{\boldsymbol{\omega}}) = \mathcal{N}(\boldsymbol{y}_t|\overline{\boldsymbol{H}}_t^T \overline{\boldsymbol{\omega}}, \overline{\boldsymbol{\Sigma}}_y) \tag{12}$$

$$p(\boldsymbol{y}_t|\underline{\boldsymbol{\omega}}) = \mathcal{N}(\boldsymbol{y}_t|\underline{\boldsymbol{H}}_t^T \underline{\boldsymbol{\omega}}, \underline{\boldsymbol{\Sigma}}_y) \tag{13}$$

The upper and lower weights can be estimated as

$$\overline{\boldsymbol{\omega}} = (\overline{\boldsymbol{H}}^T \overline{\boldsymbol{H}} + \overline{\lambda}\boldsymbol{I})^{-1} \overline{\boldsymbol{H}}^T \boldsymbol{y}_{1:T} \tag{14}$$

$$\underline{\boldsymbol{\omega}} = (\underline{\boldsymbol{H}}^T \underline{\boldsymbol{H}} + \underline{\lambda}\boldsymbol{I})^{-1} \underline{\boldsymbol{H}}^T \boldsymbol{y}_{1:T} \tag{15}$$

where $\overline{\lambda}$ and $\underline{\lambda}$ are upper and lower ridge factor.

The distribution of the upper weight $\overline{\boldsymbol{\omega}}$ and lower weight $\underline{\boldsymbol{\omega}}$ can be modeled as a Gaussian function. Let us define $\overline{\boldsymbol{\theta}} = \{\overline{\boldsymbol{\mu}}_\omega, \overline{\boldsymbol{\Sigma}}_\omega\}$ and $\underline{\boldsymbol{\theta}} = \{\underline{\boldsymbol{\mu}}_\omega, \underline{\boldsymbol{\Sigma}}_\omega\}$. Thus, the distribution of $\overline{\boldsymbol{\omega}}$ and $\underline{\boldsymbol{\omega}}$ can be represented as

$$p(\overline{\boldsymbol{\omega}}; \overline{\boldsymbol{\theta}}) = \mathcal{N}(\overline{\boldsymbol{\omega}}|\overline{\boldsymbol{\mu}}_\omega, \overline{\boldsymbol{\Sigma}}_\omega) \tag{16}$$

$$p(\underline{\boldsymbol{\omega}}; \underline{\boldsymbol{\theta}}) = \mathcal{N}(\underline{\boldsymbol{\omega}}|\underline{\boldsymbol{\mu}}_\omega, \underline{\boldsymbol{\Sigma}}_\omega) \tag{17}$$

Given a new observation state $\boldsymbol{x}_t^d = [\boldsymbol{y}_t^d, \boldsymbol{\Sigma}_y^d]$ at time t, then the mean and covariance of the conditional distribution of upper weight $p(\overline{\boldsymbol{\omega}}|\boldsymbol{x}_t^d)$ and lower weight $p(\underline{\boldsymbol{\omega}}|\boldsymbol{x}_t^d)$ can be updated as

$$\overline{\boldsymbol{\mu}}_\omega{}^* = \overline{\boldsymbol{\mu}}_\omega + \overline{\boldsymbol{K}}(\boldsymbol{y}_t^d - \overline{\boldsymbol{H}}_t{}^T \overline{\boldsymbol{\mu}}_\omega) \tag{18}$$

$$\underline{\boldsymbol{\mu}}_\omega{}^* = \underline{\boldsymbol{\mu}}_\omega + \underline{\boldsymbol{K}}(\boldsymbol{y}_t^d - \underline{\boldsymbol{H}}_t{}^T \underline{\boldsymbol{\mu}}_\omega) \tag{19}$$

$$\overline{\boldsymbol{\Sigma}}_\omega{}^* = \overline{\boldsymbol{\Sigma}}_\omega - \overline{\boldsymbol{K}}\overline{\boldsymbol{H}}_t{}^T \overline{\boldsymbol{\Sigma}}_\omega \tag{20}$$

$$\underline{\boldsymbol{\Sigma}}_\omega{}^* = \underline{\boldsymbol{\Sigma}}_\omega - \underline{\boldsymbol{K}}\underline{\boldsymbol{H}}_t{}^T \underline{\boldsymbol{\Sigma}}_\omega \tag{21}$$

where $\overline{\boldsymbol{K}} = \overline{\boldsymbol{\Sigma}}_\omega \overline{\boldsymbol{H}}_t{}^T (\boldsymbol{\Sigma}_y^d + \overline{\boldsymbol{H}}_t{}^T \overline{\boldsymbol{\Sigma}}_\omega \overline{\boldsymbol{H}}_t{}^T)^{-1}$ and $\underline{\boldsymbol{K}} = \underline{\boldsymbol{\Sigma}}_\omega \underline{\boldsymbol{H}}_t^T (\boldsymbol{\Sigma}_y^d + \underline{\boldsymbol{H}}_t{}^T \underline{\boldsymbol{\Sigma}}_\omega \underline{\boldsymbol{H}}_t{}^T)^{-1}$. The upper predicted trajectory $\overline{\boldsymbol{y}}_t^*$ and lower predicted trajectory $\underline{\boldsymbol{y}}_t^*$ can be obtained by the updated parameters of weights.

To overcome the high computation complexity of the Enhanced Karnik-Mendel (EKM) algorithm in type reduction, the adaptive factor $\boldsymbol{\alpha}$ is proposed to obtain an adaptive modulation between the upper and lower predicted trajectory.

Thus, the crisp output of the predicted trajectory can be expressed as:

$$\boldsymbol{y}_t^* = \boldsymbol{\alpha}\overline{\boldsymbol{y}}_t^* + (1 - \boldsymbol{\alpha})\underline{\boldsymbol{y}}_t^* \tag{22}$$

where the adaptive law of the factor $\boldsymbol{\alpha}$ is

$$\dot{\boldsymbol{\alpha}} = \gamma \Delta \boldsymbol{y}_t^* (\overline{\boldsymbol{y}}_t^* - \underline{\boldsymbol{y}}_t^*) \tag{23}$$

in which γ is the positive adaptation gain and $\Delta \boldsymbol{y}_t^*$ is the prediction differences of the predicted trajectory based on current observation and previous observation.

In the proposed autonomous US scanning framework, the interval iProMP is used to model the US scanning skill from demonstrations. Different from the current research on iProMP, the collaborative agents in the proposed interval iProMP are chosen as robot movement and US image information.

III. Ultrasound Image Processing

US scanning plays a vital important role in cancer diagnosis as a low-cost, noninvasive and non-ionizing radiation way to analyze the lesion tissue. In the proposed autonomous US scanning framework, US image features represent the scanning strategy in the US scanning task. It is critical to obtain the US image features to infer the US probe exploration strategy.

A. Ultrasound Image Feature Extraction

To let the robot learn the US scanning exploration strategy correctly, the US image should contain key information about anatomical structures to infer the goal of navigation. The key information of anatomical structures, such as area and location, can be extracted by image segmentation. U-Net was introduced by Olag Ronneberger and has been proven as a promising method for medical image segmentation due to precise segmentation using a scarce amount of training data [13]. In the proposed autonomous US scanning framework, to obtain the key information of anatomical structures in US images, U-Net is applied for real-time US image segmentation to infer the intention of scanning exploration. Using the pre-trained U-Net model, the predicted mask of an object will be obtained on the novel image. In the proposed autonomous US scanning framework, the image features of segmented US images are selected as area and center of gravity.

B. Ultrasound Image Quality Evaluation

During the autonomous US scanning task, the robot may navigate to a location with poor US image quality to achieve lower pose error. In order to avoid such a situation, US image quality should be considered. In the proposed autonomous US scanning framework, a confidence map is used to evaluate the US image quality during US probe navigation. The confidence map provides a stable and objective per-pixel measure of the US image quality based on the signal loss estimation method [14]. To represent the distribution of the confidence map at time t, image moment is used to describe the feature of the confidence. Thus, at time t, the US image quality can be represented by

$$c_t = \Sigma_i \Sigma_j ij C(i,j,t) \tag{24}$$

where $C(i,j,t) \in [0,1]$ denotes the pixel confidence at time t.

IV. Autonomous Ultrasound Scanning Robot System

In order to avoid any unintended injury to patients during US scanning tasks, compliance in human-robot interaction is necessary to be considered. In the proposed autonomous US scanning framework, an admittance controller is employed to ensure the compliance and safety of patients when facing an unexpected robot motion [15]. The proposed autonomous US scanning framework consists of two parts: the demonstration process and the reproduction process.

In the demonstration process, to show the US scanning strategy, the clinician will hold the end-effector of the robot to move the US probe on the tissue surface to explore the desired US image. During the US scanning demonstrated by clinicians, the US image information and robot movement will be recorded as demonstration trajectories which infer the US scanning strategy that how the robot moves based on the US image. The proposed interval iProMP is employed to learn the distribution of demonstration trajectories. The weights of demonstration trajectories are modeled by the proposed interval iProMP to correlate the image-robot movements. The workflow of the demonstration process is shown in Fig.2.

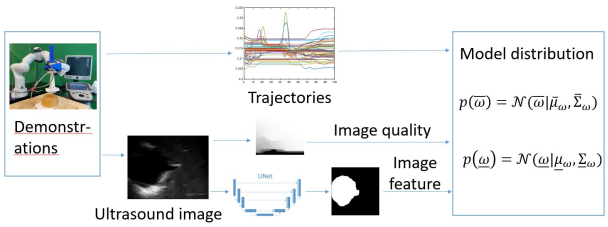

Fig. 2. Workflow of demonstration process

In the reproduction process, the US image information is observed and recognized by the model of demonstration weights. Given the current US image features, the distribution of the weight is updated to predict the intention of US image and generate the movement primitive of the robot. The updated movement primitive allows the robot to explore and realize the strategy for the US scanning task. The workflow of the reproduction process is shown in Fig.3.

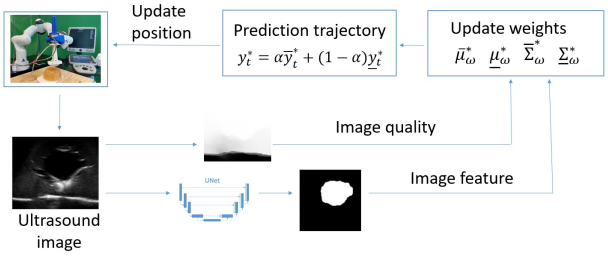

Fig. 3. Workflow of reproduction process

Compared with current research on autonomous US scanning frameworks, such as deep neural network [7] and reinforcement learning [9], the proposed framework has the advantages of lower computational complexity and time consumption. It is much easier and quicker for clinicians to transfer scanning skills to the robot after collecting scanning demonstrations.

V. Experiments and Results

In this section, we will demonstrate the feasibility and generality of the proposed autonomous US scanning toward the standard plane framework. The ability to handle the insufficient observations of the proposed interval iProMP will be evaluated in simulation.

A. Prediction Performance Evaluation in Simulation

To compare the performance of the proposed interval iProMP with traditional iProMP, the prediction results will be evaluated in simulation. Considering a breast seroma scanning scenario, we assume that the breast is in hemisphere shape and the seroma is a sphere. The task in the simulation is that the US probe could move along the breast surface and find the center of the seroma, which is shown in Fig.4. The green line represents the trajectory of the US probe. The image feature is set to be the intersection line of the section plane and the normal line through the center of US probe. To simulate different situations of seroma US scanning, the breast is set to be in different positions and rotations with different volumes of seroma. A total number of 50 demonstration trajectories is provided.

In the proposed autonomous US scanning framework, it is expected that the robot movement can be predicted based on limited observed US image information when the US probe is randomly placed on the beast surface. In this scenario, limited observation is the few US images used in the whole trajectory prediction. To evaluate the prediction performance under limited observations, the accuracy of the predicted trajectory under different observations is used to compare the prediction performance of the proposed interval iProMP and traditional iProMP. In the evaluation, the test case is that the seroma and breast are set to be in a new position

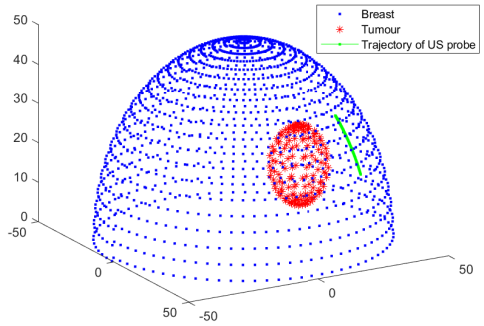

Fig. 4. Breast simulation

and rotation different from demonstrations. The root-mean-square error (RMSE) of predicted trajectories under different observations is shown in Fig.5.

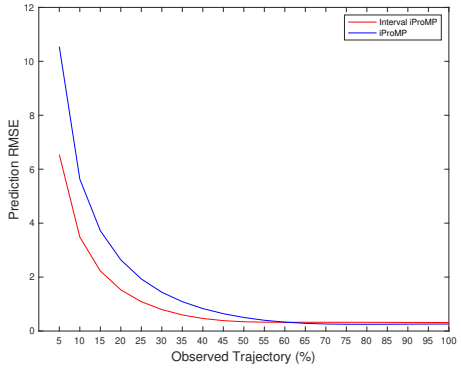

Fig. 5. Prediction Error

It can be seen that both methods have the ability to predict the trajectory under limited observations, but the prediction performance is different. When the observation is in 5% to 55%, the proposed interval iProMP achieves better prediction performance and the prediction accuracy is about 17.83 % to 45.06 % higher than iProMP. It demonstrates that the proposed interval iProMP has the potential of dealing with uncertainties in insufficient observations. When the observation is more than 60%, both methods reach the highest accuracy of predicted trajectory with similar prediction performance. It is evident that the proposed interval iProMP achieves higher prediction accuracy under limited observations.

B. Autonomous Ultrasound Scanning Experiment

We build up a US scanning robotic system using Panda robot. An Axia80-M20 force-torque sensor is mounted on its end-effector. US machine is attached to Panda robot using a 3D-printed mount. An Epiphan DVI2USB3.0 is used for real-time US image acquisition from the US probe. In this section, the localization of breast seroma is chosen as the US scanning task to validate the proposed framework. A medical phantom is used to simulate the properties of the breast with a seroma. The autonomous US scanning robot system for breast seroma is shown in Fig.6.

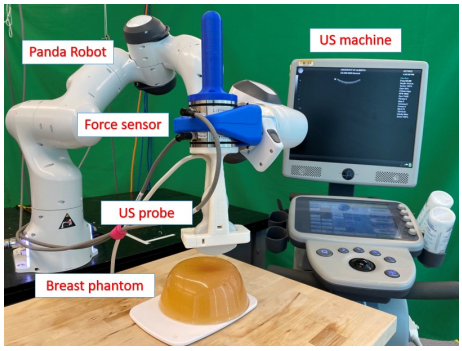

Fig. 6. US Scanning Robot System for Breast Seroma

In the proposed autonomous US scanning robot system, the US image features are extracted by the offline trained U-Net. A total number of 150 US images of breast phantom are collected to train the U-Net. The trained U-Net can realize real-time segmentation on the breast phantom. The US image quality can be evaluated by the confidence map. The segmentation results and confidence maps of the US images in different positions are shown in Fig.7.

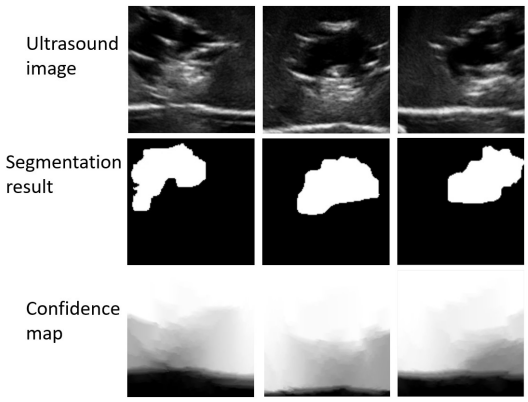

Fig. 7. US image processing results

To validate the generality of the proposed US scanning robot system for breast seroma, we assume that there is an operation area and the breast phantom can be placed anywhere within the defined operating area as shown in Fig.8. The radius of the breast phantom is about 76 mm and that of the operation area is about 114 mm. The breast seroma scanning strategy of this experiment is to let the robot automatically move the US probe to localize the seroma in the center of US image. In the demonstration process, the breast phantom is placed in different positions and rotations within the operation area, and the robot is guided to localize the seroma to the center of the US image. A total number of 25 seroma scanning demonstrations is conducted on the breast phantom.

Based on the observed US image information, the weight distribution can be updated and then predict the movement primitives of the robot. To verify the feasibility and generality

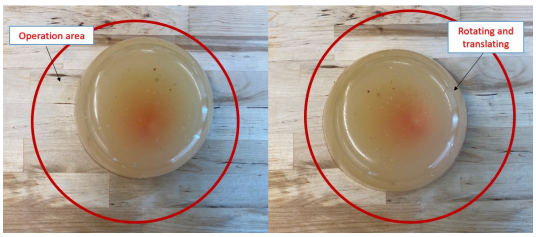

Fig. 8. Operation area

TABLE I
TESTING EXPERIMENT

Test number	1	2	3
with iProMP	77.8%(7/9)	66.7%(8/12)	73.3% (11/15)
with interval iProMP	77.8%(7/9)	83.3%(10/12)	80.0% (12/15)

of the proposed autonomous US scanning framework, in the testing process, the breast phantom will be randomly rotated and translated within the operation area. A successful autonomous US exploration means that when the US probe is randomly placed on the phantom to find the partial seroma and then the robot can automatically move the US probe to localize the seroma in the center of the US image. The testing result for performance assessment is shown in Table.I.

It can be seen that the testing experiment was in three groups: 9 tests, 12 tests, and 15 tests respectively. Each testing group was conducted separately to test the performance of the proposed method. In each test, the beast phantom was randomly placed within the operation area. It is noted that the proposed autonomous US scanning framework with both methods has the ability to realize the autonomous seroma scanning task. But the proposed framework with interval iProMP achieves a higher success rate than that with iProMP. The testing results for the seroma scanning task verified the feasibility and generality of the proposed autonomous US scanning framework. More demonstrations help to achieve higher prediction accuracy and improve the success rate. The testing performance of the proposed framework can be improved by providing more scanning demonstrations.

VI. CONCLUSION AND FUTURE WORK

In this study, we propose an autonomous US scanning towards a standard plane framework. Inspired by the FOU of IT2FS, an interval iProMP is proposed to learn the weight distribution of scanning demonstration trajectories which infers US scanning strategy. To obtain the crisp prediction output, a modulation factor α is proposed and the adaptive law is designed based on the prediction error. The US image feature can be extracted by the trained U-Net and a confidence map is used to evaluate the US image quality. The superior ability to handle the limited observations of the proposed interval iProMP is proved by the simulation result. To further validate the feasibility and generality of the proposed autonomous US scanning framework, a breast seroma scanning robot system for breast seroma scanning is set up. In the experiment, the US scanning strategy is to let the robot automatically move the US probe to localize the seroma from the edge to the center of the US image. The testing result shows the feasibility and generality of the proposed autonomous US scanning toward a standard plane framework.

There are some limitations in this work. The real-time segmentation results of the US image are not stable, which will cause the error prediction and make the sudden movement of the US probe. The other limitation is more generality is needed in this framework. Therefore, future works in this study are to obtain more stable image segmentation to ensure the scanning trajectory is smooth and safe, and increase the generality of the framework for autonomous US scanning.

REFERENCES

[1] J. Fong and M. Tavakoli, "Kinesthetic teaching of a therapist's behavior to a rehabilitation robot," in *2018 international symposium on medical robotics (ISMR)*. IEEE, 2018, pp. 1–6.

[2] Y. Liu, Y. Liu, X. Ji, L. Sun, M. Tomizuka, and X. He, "Learning from demonstration: Situation-adaptive lane change trajectory planning for automated highway driving," in *2020 IEEE International Conference on Mechatronics and Automation (ICMA)*. IEEE, 2020, pp. 376–382.

[3] X. Duan, H. Tian, C. Li, Z. Han, T. Cui, Q. Shi, H. Wen, and J. Wang, "Virtual-fixture based drilling control for robot-assisted craniotomy: Learning from demonstration," *IEEE Robotics and Automation Letters*, vol. 6, no. 2, pp. 2327–2334, 2021.

[4] V. M. Varier, D. K. Rajamani, N. Goldfarb, F. Tavakkolmoghaddam, A. Munawar, and G. S. Fischer, "Collaborative suturing: A reinforcement learning approach to automate hand-off task in suturing for surgical robots," in *2020 29th IEEE International Conference on Robot and Human Interactive Communication (RO-MAN)*. IEEE, 2020, pp. 1380–1386.

[5] K. L. Schwaner, D. Dall'Alba, P. T. Jensen, P. Fiorini, and T. R. Savarimuthu, "Autonomous needle manipulation for robotic surgical suturing based on skills learned from demonstration," in *2021 IEEE 17th International Conference on Automation Science and Engineering (CASE)*. IEEE, 2021, pp. 235–241.

[6] A. Pore, E. Tagliabue, M. Piccinelli, D. Dall'Alba, A. Casals, and P. Fiorini, "Learning from demonstrations for autonomous soft-tissue retraction," in *2021 International Symposium on Medical Robotics (ISMR)*. IEEE, 2021, pp. 1–7.

[7] X. Deng, Y. Chen, F. Chen, and M. Li, "Learning robotic ultrasound scanning skills via human demonstrations and guided explorations," *arXiv preprint arXiv:2111.01625*, 2021.

[8] Y. Huang, W. Xiao, C. Wang, H. Liu, R. Huang, and Z. Sun, "Towards fully autonomous ultrasound scanning robot with imitation learning based on clinical protocols," *IEEE Robotics and Automation Letters*, vol. 6, no. 2, pp. 3671–3678, 2021.

[9] M. Burke, K. Lu, D. Angelov, A. Straižys, C. Innes, K. Subr, and S. Ramamoorthy, "Learning rewards for robotic ultrasound scanning using probabilistic temporal ranking," *arXiv preprint arXiv:2002.01240*, 2020.

[10] A. Paraschos, C. Daniel, J. R. Peters, and G. Neumann, "Probabilistic movement primitives," *Advances in neural information processing systems*, vol. 26, 2013.

[11] G. J. Maeda, G. Neumann, M. Ewerton, R. Lioutikov, O. Kroemer, and J. Peters, "Probabilistic movement primitives for coordination of multiple human–robot collaborative tasks," *Autonomous Robots*, vol. 41, no. 3, pp. 593–612, 2017.

[12] L. A. Zadeh, "The concept of a linguistic variable and its application to approximate reasoning—i," *Information sciences*, vol. 8, no. 3, pp. 199–249, 1975.

[13] O. Ronneberger, P. Fischer, and T. Brox, "U-net: Convolutional networks for biomedical image segmentation," in *International Conference on Medical image computing and computer-assisted intervention*. Springer, 2015, pp. 234–241.

[14] A. Karamalis, W. Wein, T. Klein, and N. Navab, "Ultrasound confidence maps using random walks," *Medical image analysis*, vol. 16, no. 6, pp. 1101–1112, 2012.

[15] M. T. Mason, "Compliance and force control for computer controlled manipulators," *IEEE Transactions on Systems, Man, and Cybernetics*, vol. 11, no. 6, pp. 418–432, 1981.